Pion and muon production in e^-, e^+, γ plasma

Inga Kuznetsova,[1] Dietrich Habs,[2] and Johann Rafelski[1,2]
[1]*Department of Physics, University of Arizona, Tucson, Arizona, 85721, USA*
[2]*Department für Physik der Ludwig-Maximilians-Universität München und Maier-Leibnitz-Laboratorium, Am Coulombwall 1, 85748 Garching, Germany*
(Received 25 March 2008; published 31 July 2008)

We study production and equilibration of pions and muons in relativistic electron-positron-photon plasma at a temperature of $T \ll m_\mu, m_\pi$. We argue that the observation of pions and muons can be a diagnostic tool in the study of the initial properties of such a plasma formed by means of strong laser fields. Conversely, properties of muons and pions in a thermal environment become accessible to precise experimental study.

DOI: 10.1103/PhysRevD.78.014027 PACS numbers: 13.60.Le, 52.27.Ny, 33.20.Xx

I. INTRODUCTION

The formation of a relativistic (temperature T in the MeV range) electron-positron-photon e^-, e^+, γ plasma (EP^3) in the laboratory using ultrashort pulse lasers is one of the topics of current interest and forthcoming experimental effort [1,2]. The elementary properties of EP^3 have recently been reported (see [3]) where typical properties are explicitly presented for $T = 10$ MeV. One of the challenges facing a study of EP^3 will be the understanding of the fundamental mechanisms leading to its formation. We propose here as a probe the production of heavy particles with mass $m \gg T$. Clearly, these processes occur during the history of the event at the highest available temperature, and thus information about the early stages of the plasma, and even the preequilibrium state, should become accessible in this way.

We focus our attention on the strongly interacting pions $\pi^\pm$, π^0 ($m_\pi c^2 \lesssim 140$ MeV), and muons $\mu^\pm (m_\mu c^2 \lesssim 106$ MeV) (*in the following we use units in which* $k = c = \hbar = 1$, *and thus we omit these symbols from all equations. Both the particle mass and plasma temperature are thus given in the energy unit MeV.*) These very heavy, compared to the electron ($m_e c^2 = 0.511$ MeV), particles are, as noted, natural "deep" diagnostic tools of the EP^3 drop. Of special interest is the neutral pion π^0 which is, among all other heavy particles, most copiously produced for $T \ll m$. The π^0 yield and spectrum will be therefore of great interest in the study of the EP^3 properties. Conversely, the study of the in-medium pion mass splitting $\Delta m = m_{\pi^\pm} - m_{\pi^0} = 4.594$ MeV at a temperature $T \gtrsim \Delta m$ will contribute to the better understanding of this relatively large mass splitting between π^0 and $\pi^\pm$, $\Delta m/\bar{m} = 3.34\%$, believed to originate in the isospin symmetry breaking electromagnetic radiative corrections.

However, given its very short natural lifespan,

$$\pi^0 \to \gamma + \gamma, \qquad \tau^0_{\pi^0} = (8.4 \pm 0.6)10^{-17} \text{ s}.$$

π^0 is also the particle most difficult to experimentally study among those we consider: its decay products reach the detection system nearly at the same time as the electromagnetic energy pulse of the decaying plasma fireball, which is likely to "blind" the detectors.

This plasma drop we consider is up to a thousand times hotter than the center of the sun. This implies the presence of the corresponding high particle density n, energy density ϵ, and pressure P. These quantities in the plasma can be evaluated using the relativistic expressions

$$n_i = \int g_i f_i(p) d^3p, \tag{1}$$

$$\epsilon = \int \sum_i g_i E_i f_i(p) d^3p, \qquad E_i = \sqrt{m_i^2 + \vec{p}^2}, \tag{2}$$

$$P = \frac{1}{3} \int \sum_i g_i \left(E_i - \frac{m_i^2}{E_i}\right) f_i(p) dp^3, \tag{3}$$

where subscript $i \in \gamma, e^-, e^+, \pi^0, \pi^+, \pi^-, \mu^-, \mu^+$, $f_i(p)$ is the momentum distribution of the particle i and g_i its degeneracy; for $i = e^-, e^+, \gamma, \mu^-, \mu^+$ we have $g_i = 2$; and $g_i = 1$ for π^0, π^-, π^+. For a QED plasma which lives long enough so that electrons and positrons are in thermal and chemical equilibrium with photons, ignoring small QED interaction effects, we use Fermi and Bose momentum distribution, respectively:

$$f_{e^\pm} = \frac{1}{e^{(u\cdot p_e \pm \nu_e)/T} + 1}, \qquad f_\gamma = \frac{1}{e^{u\cdot p_\gamma/T} - 1}. \tag{4}$$

The invariant form comprises the Lorentz-scalar $u \cdot p_e$, a scalar product of the particle four-momentum p_i^μ with the local four-vector of velocity u^μ. In the absence of matter flow and in the rest (in the laboratory) frame we have

$$u^\mu = (1, \vec{0}), \qquad p_i^\mu = (E_i, \vec{p}_i). \tag{5}$$

When the electron chemical potential ν_e is small, $\pi T \gg \nu_e$, the number of particles and antiparticles is the same, $n_{e^-} = n_{e^+}$. Physically, it means that the number of e^+e^- pairs produced is dominating residual matter electron yield. This is the case for all laboratory experimental

environments of interest here, in which $T > 2$ MeV is achieved. We thus will set $\nu_e = 0$ in the following.

It is convenient to parametrize the electron, positron, and photon e^-, e^+, γ plasma properties in terms of the properties of the Stephan-Boltzmann law for massless particles (photons), presenting the physical properties in terms of the effective degeneracy $g(T)$ comprising the count of all particles present at a given temperature T:

$$\frac{\mathcal{E}}{V} = \epsilon = g(T)\sigma T^4, \qquad 3P = g'(T)\sigma T^4, \qquad \sigma = \frac{\pi^2}{30}. \tag{6}$$

For temperatures $T \ll m_e$ we only have in this case truly massless photons and $g(T) \simeq g'(T) \simeq 2_\gamma$. Once temperature approaches and increases beyond m_e, we find $g \simeq g'(T) \simeq 2_\gamma + (7/8)(2_{e^-} + 2_{e^+}) = 5.5$ degrees of freedom. In principle these particles acquire additional in-medium mass which reduces the degree of freedom count, but this effect is compensated by collective "plasmon" modes; thus we proceed with naive counting of nearly free EP[3] components. The factor of $7/8$ expresses the difference in the evaluation of Eq. (3) for the momentum distribution of Fermions and Bosons in Eq. (4), with Bosons providing the reference point at low T, where only massless photons are present. In passing, we note that in the early Universe there would be further present the neutrino degrees of freedom, not considered here for the laboratory experiments, considering their weak coupling to matter.

In Fig. 1 we present both $g(T)$ and $g'(T)$, as a function of temperature T in the form of the energy density ϵ normalized by σT^4, and, respectively, the pressure P, normalized by $\sigma T^4/3$. The $g(T)$ jumps more rapidly compared to $g'(T)$, between the limiting case of a black body photon gas at $T < 0.5$ MeV ($g = 2$) and the case $g = 5.5$ for γ, e^-, e^+, since the energy density also contains the rest mass energy content of all particles present. The rise of the ratio at $T > 15$ MeV indicates the contribution of the excitation of muons and pions in equilibrated plasma. We note that the plasma-produced pions (and muons) are in general not in chemical equilibrium. The distribution functions which maximize entropy content at a given particle number and energy content are [4]

$$f_\pi = \frac{1}{\Upsilon_{\pi^0(\pi^\pm)}^{-1} e^{u\cdot p_\pi/T} - 1}, \qquad f_\mu = \frac{1}{\Upsilon_\mu^{-1} e^{u\cdot p_\mu/T} + 1}, \tag{7}$$

where $\Upsilon_{\pi^0(\pi^\pm)}$ and Υ_μ are particles fugacities. For $\Upsilon_i \to 0$ the quantum distributions shown in Eq. (7) turn into the classical Boltzmann distributions, with the abundance prefactor Υ_i.

In the case of interest here, when $T < m$, it suffices to consider the Boltzmann limit of the quantum distributions

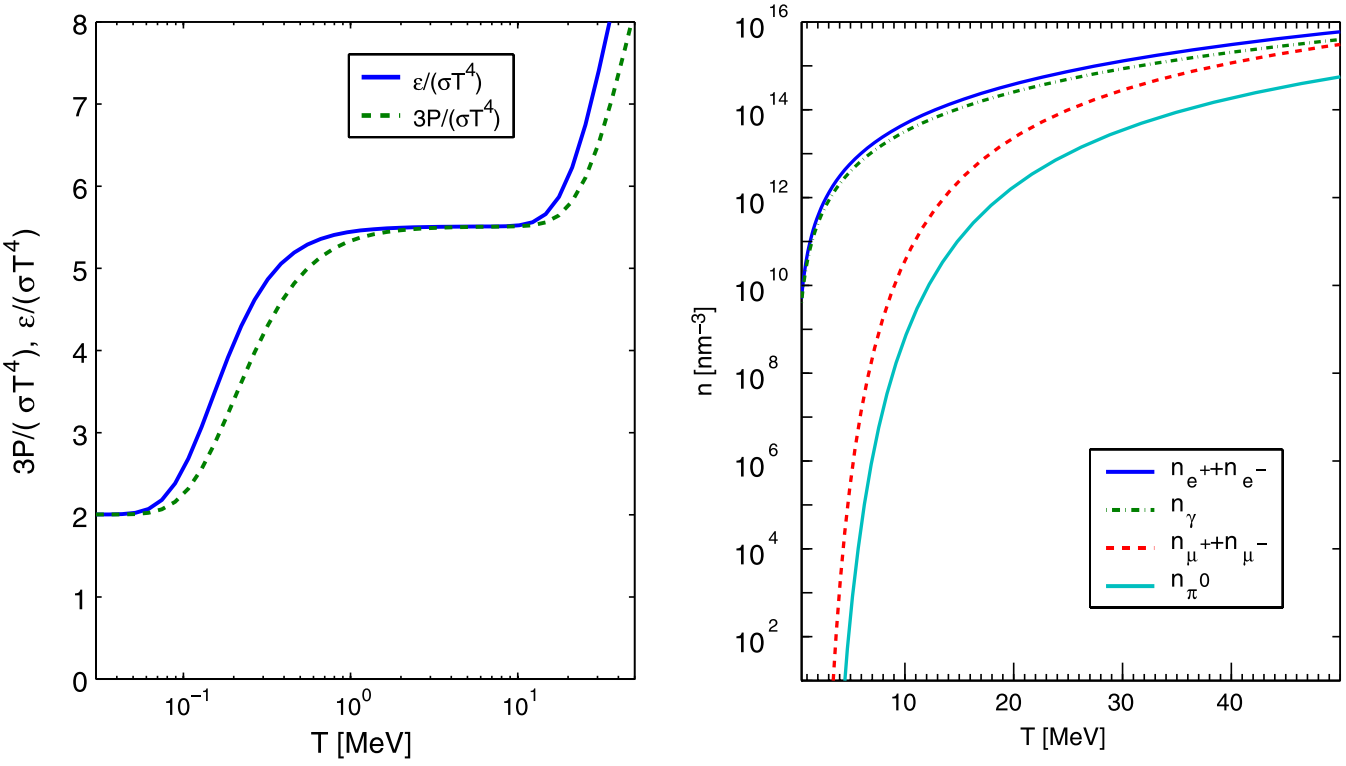

FIG. 1 (color online). On the left: the ratios $g \equiv \epsilon/\sigma T^4$ and $g' \equiv 3P/\sigma T^4$ as a function of temperature T; on the right: the equilibrium densities of electrons (top blue solid line), photons (green dash-dotted line), muons (red dashed line), pions (bottom blue solid line) as functions of temperature T.

in Eq. (7), that is, to drop the "one" in the denominator. Using the Boltzmann momentum distribution and taking the nonrelativistic limit we have

$$\frac{N_\pi}{V} \equiv n_\pi = \Upsilon_\pi \frac{1}{2\pi^2} T m_\pi^2 K_2(m_\pi/T) \rightarrow \Upsilon_\pi \left(\frac{m_\pi T}{2\pi}\right)^{3/2} e^{-m_\pi/T} + \ldots, \quad (8)$$

where K_2 (and further below also K_1) are the modified Bessel functions of integer order "2" (and "1," respectively).

The particle densities are shown on the right in Fig. 1. The top solid line is the sum of $n_{e^+} + n_{e^-}$, which is bigger than the photon density (dash-dotted, green) which follows below. We also include in the figure the sum density of muons $n_{\mu^+} + n_{\mu^-}$ (dashed line, red), and the density of the neutral pion π^0 (bottom solid line). The chemical equilibrium corresponds to $\Upsilon_{\pi^0(\pi^\pm)} = \Upsilon_\mu = 1$ and is used on the right in Fig. 1, since this is the maximum density that can be reached in the buildup of these particles, for a given temperature. Both heavy particle densities appear comparatively small in the temperature range of interest. However, in magnitude they rival the normal atomic density ($\simeq 10^2/\text{nm}^3$) already at $T = 4$ MeV, and 5 MeV, respectively. This high particle density in the chemically equilibrated plasma explains the relatively large collision and reaction rates we obtain in this work. In turn, this opens the question of how such a dense, chemically equilibrated EP^3 state can be formed—we observe that colliding two ultraintense circularly polarized and focused laser beams on a heavy thin metal foil(s) is the current line of approach. Initial simulations were performed [5]. Many strategies can be envisaged aiming to deposit the laser pulse energy in the smallest possible spatial and temporal volume, and this interesting and challenging topic will without doubt keep us and others busy in years to come.

As it turns out, even a small drop of EP^3 plasma with a size scale of 1 nm is, given the high particle density, opaque. The mean free paths l_i of particles " i" are relatively short, at subnanoscale [3]:

$$l_e \simeq \left(\frac{10\ \text{MeV}}{T}\right)^3 \left(\frac{E}{31.1\ \text{MeV}}\right)^2 0.37\ \text{nm}, \qquad l_\gamma \simeq \left(\frac{10\ \text{MeV}}{T}\right)^2 \left(\frac{E}{27.5\ \text{MeV}}\right) 0.28\ \text{nm}, \quad (9)$$

where the reference energy values (31.1 and 27.5 MeV) correspond to the mean particle energy at $T = 10$ MeV. Photons are subject to Compton scattering, and electrons and positrons to charged particle scattering. In fact these values of l_i are likely to be upper limits, since Bremsstrahlung type processes are believed to further increase opaqueness of the plasma [6]. In our considerations plasma particles of energy above 70 MeV are of interest, since these are responsible for the production of heavy particles. We see that the mean free path of such particles has also a nanometer scale magnitude.

We note that an EP^3 drop of radius 2 nm at $T = 10$ MeV contains 13 kJ energy. This is the expected energy content of a light pulse at ELI (European Light Infrastructure, in development) with a pulse length of about $\Delta t = 10^{-14}$ s. For comparison, the maximum energy available in particle accelerators for at least 20, if not more, years will be in head-on Pb–Pb central collisions at LHC at CERN, in its LHC-ion collider mode, where per nucleon energy of about 3 TeV is reached. Thus the total energy available is 200 μJ, of which about 10%–20% becomes thermalized. Thus ELI will already have an overall energy advantage of 10^9, while in the LHC-ion case the great advantages are (a) the natural localization of the energy at the length scale of 10^{-5} nm, given that the energy is contained in colliding nuclei, and (b) the high repetition rate of collisions.

As a purely academic exercise, we note that should one find a way to "focus" the energy in ELI to nuclear dimensions, and scaling the energy density with T^4 up from what is expected to be seen at the CERN LHC ion ($T < 1$ GeV), one would exceed $T = 150$ GeV, the presumed electroweak phase boundary. Such a consideration leads the authors of Refs. [1,2] to suggest that the electroweak transition may be achieved at some future time using ultrashort laser pulses.

Returning to present-day physics, we are assuming here that T near and in MeV range is achievable in the foreseeable future, and that much higher values are obtainable in the presence of pulses with $\Delta t < 10^{-18}$ s, $c\Delta t < 0.3$ nm. Hence we consider production processes for π^0, $\pi^\pm$, $\mu^\pm$ for $T < 50$ MeV. We study here all two body reactions in EP^3 which lead to the formation of the particles of interest, excluding solely $e\gamma \rightarrow e\pi^0$, and the related $e^-e^+ \rightarrow \gamma\pi^0$. The presence of a significant (1.2%) fraction of $\pi^0 \rightarrow e^+e^-\gamma$ decays implies that these related two body processes could be important in our considerations. However, these reactions involve the π^0 off-mass shell coupling to two photons, which needs to be better understood before we can consider these reactions in our context.

We also do not consider here the inverse three body reactions $e^+e^-\gamma \rightarrow \pi^0$, since there is no exponential gain in using $n > 2$ particles to overcome an energy threshold, here m_{π^0}. The independent probability of finding n particles with energy m_{π^0}/n each is the same for any value of n:

$$P_1 P_2 \ldots P_n \propto (e^{-m_{\pi^0}/nT})^n = e^{-(m_{\pi^0}/T)}. \quad (10)$$

This resolves the argument that more particles could more easily overcome the reaction barrier. n-body reactions with $n > 2$ are in fact suppressed in EP^3 by the weakness of the electromagnetic (EM) interaction, since adding an EM-interacting particle to the reactions process requires an EM vertex with $\alpha = 1/137$. Thus microscopic reactions in EP^3 involving $n > 2$ are suppressed by a factor of 100

for each additional EM particle involved in the reaction. This does not mean that a collective/coherent process of heavy particle production by many particles is similarly suppressed: for example, fast time varying electromagnetic fields provide through $\vec{E}\cdot\vec{B}$ a collective source of π^0. We defer further study of this production mechanism which requires multi-MeV^{-1} range oscillation to be present in EP^3.

In the following section, we introduce the master equation governing the production of pions and muons in plasma and formulate the invariant rates in terms of known physical reactions. In Sec. III we obtain the numerical results for particle production rates and reaction relaxation times which we present as figures. In Sec. IV we discuss these results further and consider their implications.

II. PARTICLE PRODUCTION RATES

A. π^0 production

π^0 in the QED plasma is produced predominantly in the thermal two photon fusion [7]:

$$\gamma + \gamma \rightarrow \pi^0. \tag{11}$$

Much less probable is the production of π^0 in the reaction:

$$e^- + e^+ \rightarrow \pi^0. \tag{12}$$

These formation processes are the inverse of the decay process of π^0. The smallness of the electroformation of π^0 is characterized by the small branching ratio in π^0 decay $B = \Gamma_{ee}/\Gamma_{\gamma\gamma} = (6.2 \pm 0.510^{-8})$. Other decay processes involve more than two particles. π^0 can also be formed by charged pions in charge exchange reactions. However, in EP^3 in the domain of the T of interest we find that at first the neutral pions will be produced. These in turn produce charged pions. Therefore we introduce the pion charge exchange process in the context of charged pion formation in the subsection II C, and since it can be important, we show it explicitly here as well.

Omitting all subdominant processes, the resulting master equation for neutral pion number evolution is

$$\frac{1}{V}\frac{dN_{\pi^0}}{dt} = \frac{d^4W_{\gamma\gamma\to\pi^0}}{dVdt} - \frac{d^4W_{\pi^0\to\gamma\gamma}}{dVdt} + \frac{d^4W_{\pi^+\pi^-\to\pi^0+\pi^0}}{dVdt} - \frac{d^4W_{\pi^0\pi^0\to\pi^+\pi^-}}{dVdt}, \tag{13}$$

where N_{π^0} is the total number of π^0, V is the volume of the system, $d^4W_{\gamma\gamma\to\pi^0}/dVdt$ is the (Lorentz) invariant π^0 production rate per unit time and volume in photon fusion, and $d^4W_{\pi^0\to\gamma\gamma}/dVdt$ is the invariant π^0 decay rate per unit volume and time. Similarly, $d^4W_{\pi^+\pi^-\to\pi^0\pi^0}/dVdt$ is the pion charge exchange π^0 production rate per unit time and volume, while $d^4W_{\pi^0\pi^0\to\pi^+\pi^-}/dVdt$ is the corresponding reverse reaction loss rate.

We assume that in the laboratory frame the momentum distribution of produced π^0 is characterized by the ambient temperature. Equation (8) defines the relation of fugacity Υ_π to the yield. This equation allows now the study of the production dynamics as if we were dealing with a π^0 in a thermal bath, and to exploit the detailed balance between decay and production process in order to estimate the rate of π^0 production. This theoretical consideration should not be understood as an assumption of the equilibration of π^0, which could upon production escape from the small plasma drop.

In [7] the detailed balance relation is derived in detail, which takes the form

$$\Upsilon_{\pi^0}^{-1}\frac{d^4W_{\pi^0\to\gamma\gamma}}{dVdt} = \Upsilon_\gamma^{-2}\frac{d^4W_{\gamma\gamma\to\pi^0}}{dVdt} \equiv R_{\pi^0}. \tag{14}$$

This allows that Eq. (13) can be written in the form

$$\frac{1}{V}\frac{dN_{\pi^0}}{dt} = (\Upsilon_\gamma^2 - \Upsilon_{\pi^0})R_{\pi^0} - (\Upsilon_{\pi^0}^2 - \Upsilon_{\pi^\pm}^2)R_{\pi^0\pi^0\leftrightarrow\pi^+\pi^-}. \tag{15}$$

For $\Upsilon_{\pi^0} \rightarrow \Upsilon_\gamma^2 \rightarrow \Upsilon_{\pi^\pm}^2 = 1$ we reach chemical equilibrium; the time variation of density due to production and decay vanishes.

The charge exchange process rate [$R_{\pi^0\pi^0\leftrightarrow\pi^+\pi^-}$, last in Eq. (15)] balances the first contribution in Eq. (44), where it will be further discussed. The rate R_{π^0} can be written as

$$\begin{aligned} R_{\pi^0} = {} & \int\frac{d^3p_\pi}{(2\pi)^3 2E_\pi}\int\frac{d^3p_{2\gamma}}{(2\pi)^3 2E_{2\gamma}}\int\frac{d^3p_{1\gamma}}{(2\pi)^3 2E_{1\gamma}} \\ & \times (2\pi)^4\delta^4(p_{1\gamma} + p_{2\gamma} - p_\pi) \\ & \times \sum_{\text{spin}}|\langle p_{1\gamma}p_{2\gamma}|M|p_\pi\rangle|^2 f_\pi(p_\pi)f_\gamma(p_{1\gamma})f_\gamma(p_{2\gamma}) \\ & \times \Upsilon_\gamma^{-2}\Upsilon_{\pi^0}^{-1}e^{u\cdot p_\pi/T}, \end{aligned} \tag{16}$$

where for π^0 formation there was the factor $(1 + f_\pi)$ which we reduced using the relation

$$1 \mp f_\pm = \Upsilon_i^{-1}e^{u\cdot p_i/T}f_\pm, \tag{17}$$

where Fermi (f_+) and Bose (f_-) distributions are implied for particle i. Similarly, in the π^0 decay case we replaced the two stimulated decay factors $(1 + f_\gamma)^2$ in that way. Equation (16) follows. Including in Eq. (16) the prefactors required by Eq. (14) and recalling time reversal invariance, i.e., $M = M^\dagger$,

$$|\langle p_{1\gamma}p_{2\gamma}|M|p_\pi\rangle|^2 = |\langle p_\pi|M|p_{1\gamma}p_{2\gamma}\rangle|^2. \tag{18}$$

We realize that the result, Eq. (16), is manifestly symmetric for the two reaction directions. It is interesting to note that in the Boltzmann limit all fugacities cancel in Eq. (16).

We introduce the pion equilibration (relaxation) time constant by

$$\tau_{\pi^0} = \frac{dn_{\pi^0}/d\Upsilon_{\pi^0}}{R_{\pi^0}}. \tag{19}$$

Note that when the volume does not change in time on a scale of τ_{π^0} (absence of expansion dilution) and thus T is constant, the left-hand side of Eq. (15) becomes dn_{π^0}/dt. Given the relaxation time definition of Eq. (19) the time evolution of the pion fugacity for a system at fixed time independent temperature satisfies

$$\tau_{\pi^0}\frac{d\Upsilon_{\pi^0}}{dt} = \Upsilon_\gamma^2 - \Upsilon_{\pi^0} - (\Upsilon_{\pi^0}^2 - \Upsilon_{\pi^\pm}^2)\frac{R_{\pi^0\pi^0\leftrightarrow\pi^+\pi^-}}{R_{\pi^0}}. \tag{20}$$

When the charge exchange reaction can be ignored, for $\Upsilon_{\pi^0}(t=0)=0$ we find the analytical solution $\Upsilon_{\pi^0} = \Upsilon_\gamma^2(1-e^{-t/\tau_{\pi^0}})$, justifying the proposed definition of the relaxation constant.

We note that Eq. (20) also describes the decay of a π^0. Therefore, up to small modifications introduced by the thermal medium (see discussion below),

$$\tau_{\pi^0} \simeq \tau^0_{\pi^0}.$$

The π^0 production rate is thus related to the decay rate $1/\tau^0_{\pi^0}$ by the simple formula

$$R_{\pi^0} \simeq \frac{dn_{\pi^0}/d\Upsilon_{\pi^0}}{\tau^0_{\pi^0}} \simeq \left(\frac{m_\pi T}{2\pi}\right)^{3/2}\frac{e^{-m_\pi/T}}{\tau^0_{\pi^0}}, \tag{21}$$

where in the last expression we have used Eq. (8) in the limit $m \gg T$. It is important for the reader to remember that derivation of Eq. (21) is based on detailed balance in thermally equilibrated plasma, and does not require chemical equilibrium to be established.

Now we consider how and why $\tau_{\pi^0} \simeq \tau^0_{\pi^0}$. It turns out that there are both relativistic and quantum effects which contribute and they (nearly) cancel: the relativistic effect arises because τ_{π^0} in Eq. (21) is in the lab frame while the known $\tau^0_{\pi^0}$ is in the pion rest frame. In the relativistic Boltzmann limit the correction is obtained considering the related time dilation effect [7] is

$$\tau_{\pi^0} = \frac{\tau^0_{\pi^0}}{\langle 1/\gamma\rangle} = \tau^0_{\pi^0}\frac{K_2(m_{\pi^0}/T)}{K_1(m_{\pi^0}/T)}, \tag{22}$$

where $\langle 1/\gamma\rangle$ is the average inverse Lorentz factor. We find that this effect implies that τ_{π^0} in the lab frame increases with temperature. This effect is shown by a dashed (blue) line in Fig. 2. Furthermore, with increasing temperature quantum distribution functions for photons and for the produced particle need to be considered. This leads to the result shown as a solid line (green) in Fig. 2. Thus in general $\tau_{\pi^0} > \tau^0_{\pi^0}$, by up to 14%.

We can further evaluate exactly the reaction rate of Eq. (16) [7]:

$$R_{\pi^0} = \frac{1}{(2\pi)^2}\frac{m_\pi}{\tau^0_{\pi^0}}\int_0^\infty \frac{p_\pi^2 dp_\pi}{E_\pi}\frac{\Upsilon_{\pi^0}^{-1}e^{E_\pi/T}}{\Upsilon_{\pi^0}^{-1}e^{E_\pi/T}-1}\Phi(p_\pi), \tag{23}$$

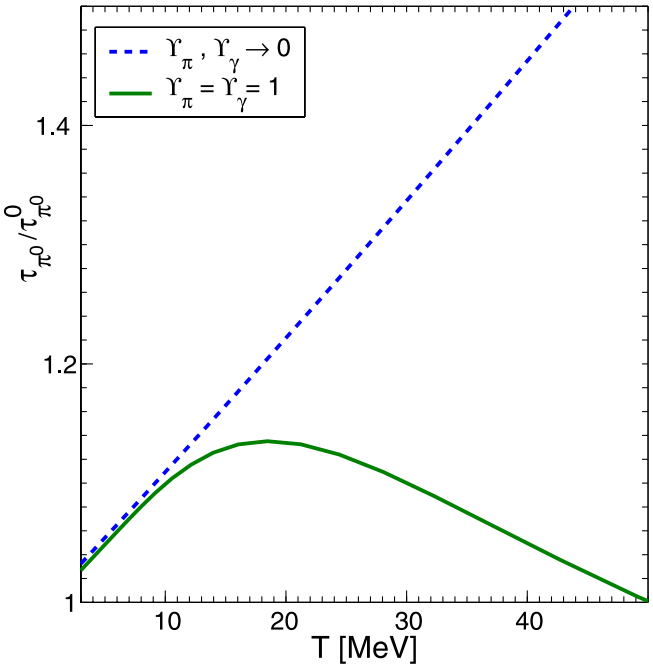

FIG. 2 (color online). The ratios $\tau_{\pi^0}/\tau^0_{\pi^0}$ as functions of temperature T for the relativistic Boltzmann limit (blue dashed line) and for quantum distribution in chemical equilibrium, $\Upsilon_\pi = \Upsilon_\gamma = 1$ (green solid line).

where

$$\Phi(p_\pi) = \int_{-1}^{1} d\zeta \Upsilon_\gamma^{-2}\frac{1}{\Upsilon_\gamma^{-1}e^{(a-b\zeta)}-1}\frac{1}{\Upsilon_\gamma^{-1}e^{(a+b\zeta)}-1}, \tag{24}$$

with

$$a = \frac{\sqrt{m_\pi^2+p_\pi^2}}{2T}; \qquad b = \frac{p_\pi}{2T}. \tag{25}$$

This integral for $\Upsilon_\gamma = 1$ takes the form

$$\Phi(p_{\pi^0}) = \frac{2}{b(e^{2a}-1)}\left(b + \ln\left(1+\frac{(e^{(b-a)}-e^{-(a+b)})}{(1-e^{b-a})}\right)\right). \tag{26}$$

This exact result (solid line, blue) is compared to the approximate result of Eq. (21) (dashed line, green) in Fig. 3. We note that it is hard to discern a difference on logarithmic scale, especially so for small temperatures where the only (small) effect is the relativistic time dilation. This implies that it is appropriate to use the simple result of Eq. (21) in the study of π^0 production.

Before closing this section we note that we can use exactly the same method to extract from the partial width of the $\pi^0 \to e^+e^-$ the reaction rate for the inverse process, which will be discussed below. All arguments carry through in identical and exact fashion replacing where

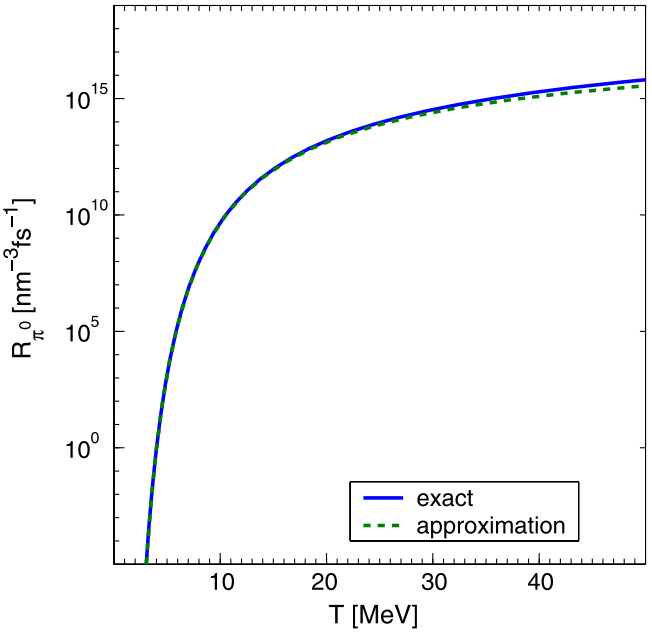

FIG. 3 (color online). The π^0 production rate (blue solid line) and approximate rate from Eq. (21) (green dashed line) as functions of temperature T.

appropriate the Bose by Fermi distributions and using Eq. (17).

B. Muon production

In the plasma under consideration, muons can be directly produced in the reactions:

$$\gamma + \gamma \rightarrow \mu^+ + \mu^-, \tag{27}$$

$$e^+ + e^- \rightarrow \mu^+ + \mu^-. \tag{28}$$

For reactions (27) and (28) the master evolution equation developed for the study of thermal strangeness in heavy ion collisions applies [8–11] [compared to these references our definition is changed; their $R_{12\rightarrow 34} \rightarrow R_{12\rightarrow 34}/(\Upsilon_1\Upsilon_2)$ in order to make the forward-backward symmetry explicit]

$$\frac{1}{V}\frac{dN_\mu}{dt} = (\Upsilon_\gamma^2 - \Upsilon_\mu^2)R_{\gamma\gamma\leftrightarrow\mu^+\mu^-} + (\Upsilon_e^2 - \Upsilon_\mu^2)R_{e^+e^-\leftrightarrow\mu^+\mu^-}. \tag{29}$$

Like before for π^0 we consider the master equation in order to find an appropriate definition of the relaxation time constant for $\mu^\pm$ production. In no way should this be understood to imply that muons are retained in the small plasma drop. In chemically equilibrated EP[3] the μ production relaxation time is defined by

$$\tau_\mu = \frac{1}{a}\frac{dn_\mu/d\Upsilon_\mu}{(R_{\gamma\gamma\leftrightarrow\mu^+\mu^-} + R_{e^+e^-\leftrightarrow\mu^+\mu^-})}, \tag{30}$$

where a suitable choice is $a = 1$, 2 for $t = 0$, ∞, respectively (see below). The form of Eq. (30) ensures that, omitting the volume expansion, i.e., the dilution effect, the evolution of the muon fugacity obeys the equation

$$a\tau_\mu\frac{d\Upsilon_\mu}{dt} = 1 - \Upsilon_\mu^2, \qquad \Upsilon_\gamma = \Upsilon_e = 1, \tag{31}$$

which has for $\Upsilon_\mu(t = 0) = 0$ the simple analytical solution [9]

$$\Upsilon_\mu = \tanh t/a\tau_\mu. \tag{32}$$

For $t \rightarrow \infty$, near to chemical equilibrium, $\Upsilon_\mu \rightarrow 1 - e^{-2t/a\tau_\mu}$, while for $t \rightarrow 0$, at the onset of particle production with small Υ_μ, we have $\Upsilon_\mu = t/(a\tau_\mu)$. Hence, near to chemical equilibrium it is appropriate to use $a = 2$ in the definition of relaxation time of Eq. (30), while at the onset of particle production, more applicable to this work a more physical choice would be $a = 1$. However, following the convention, in the results presented below the value $a = 2$ is used.

The invariant muon production rate in photon fusion as introduced above is

$$R_{\gamma\gamma\leftrightarrow\mu^+\mu^-} = \int\frac{d^3p_{\mu^+}}{(2\pi)^3 2E_{\mu^+}}\int\frac{d^3p_{\mu^-}}{(2\pi)^3 2E_{\mu^-}}\int\frac{d^3p_{1\gamma}}{(2\pi)^3 2E_{1\gamma}}\int\frac{d^3p_{2\gamma}}{(2\pi)^3 2E_{2\gamma}}(2\pi)^4\delta^4(p_{1\gamma} + p_{2\gamma} - p_{\mu^+} - p_{\mu^-}) \times \sum_{\text{spin}}|\langle p_{1\gamma}p_{2\gamma}|M_{\gamma\gamma\rightarrow\mu^+\mu^-}|p_{\mu^+}p_{\mu^-}\rangle|^2 f_\gamma(p_{1\gamma})f_\gamma(p_{2\gamma})f_\mu(p_{\mu^+})f_\mu(p_{\mu^-})\Upsilon_\gamma^{-2}\Upsilon_\mu^{-2}e^{u\cdot(p_{\mu^+}+p_{\mu^-})/T}, \tag{33}$$

and the invariant muon production rate in electron-positron fusion is

$$R_{e^+e^-\leftrightarrow\mu^+\mu^-} = \int\frac{d^3p_{\mu^+}}{(2\pi)^3 2E_{\mu^+}}\int\frac{d^3p_{\mu^-}}{(2\pi)^3 2E_{\mu^-}}\int\frac{d^3p_{e^+}}{(2\pi)^3 2E_{e^+}}\int\frac{d^3p_{e^-}}{(2\pi)^3 2E_{e^-}}(2\pi)^4\delta^4(p_{e^+} + p_{e^-} - p_{\mu^+} - p_{\mu^-}) \times \sum_{\text{spin}}|\langle p_{e^+}p_{e^-}|M_{e^+e^-\rightarrow\mu^+\mu^-}|p_{\mu^+}p_{\mu^-}\rangle|^2 f_e(p_{e^+})f_e(p_{e^-})f_\mu(p_{\mu^+})f_\mu(p_{\mu^-})\Upsilon_e^{-2}\Upsilon_\mu^{-2}e^{u\cdot(p_{\mu^+}+p_{\mu^-})/T}. \tag{34}$$

We note that in Eqs. (33) and (34) in the Boltzmann limit all fugacities cancel, and that the forward-backward reaction symmetry is explicit. Moreover, it is interesting to note that despite inclusion of quantum effects (Bose stimulated emission

and/or Fermi blocking), when using rates as defined in this paper, we do not change the master population equation system arising for Boltzmann particles. The only modification is a slight fugacity dependence of rates presented in Eqs. (16), (33), and (34).

The $\sum |M_{e^+e^-\to\mu^+\mu^-}|^2$ differs from often considered heavy quark production $\sum |M_{q\bar{q}\to c\bar{c}}|^2$ [12,13] ($m_c \gg m_q$) by color factor 2/9, and the coupling $\alpha_s \to \alpha$ of QCD has to be changed to $\alpha = 1/137$ of QED. Then we obtain, based on the above references,

$$\sum |M_{e^+e^-\to\mu^+\mu^-}|^2 = g_e^2 8\pi^2\alpha^2 \times \frac{(m^2-t)^2+(m^2-u)^2+2m^2s}{s^2}, \tag{35}$$

where $m = 106$ MeV is the muon mass; the electron and positron degeneracy is $g_e = 2$; the s, t, u are the usual Mandelstam variables: $s = (p_1+p_2)^2$, $t = (p_3-p_1)^2$, $u = (p_3-p_2)^2$, $s+t+u = 2m^2$. For the total averaged over initial states $|M|^2$ for photon fusion we have

$$|M_{\gamma\gamma\to\mu^+\mu^-}|^2 = g_\gamma^2 8\pi^2\alpha^2\left(-4\left(\frac{m^2}{m^2-t}+\frac{m^2}{m^2-u}\right)^2 + 4\left(\frac{m^2}{m^2-t}+\frac{m^2}{m^2-u}\right) + \frac{m^2-u}{m^2-t} + \frac{m^2-t}{m^2-u}\right), \tag{36}$$

where degeneracy $g_\gamma = 2$. Near threshold $s \approx 4m^2$, with t, $u \approx -m^2$ we find

$$|M_{\gamma\gamma\to\mu^+\mu^-}|^2 = 64\pi^2\alpha^2, \qquad |M_{e^+e^-\to\mu^+\mu^-}|^2 = 32\pi^2\alpha^2. \tag{37}$$

The $e^+e^- \to \mu^+\mu^-$ reaction involves a single photon, and thus it is more constrained (by a factor of 2) compared to the photon fusion, which is governed by two Compton type Feynman diagrams. However, in the rate we compute below, the indistinguishability of the two photons introduces an additional factor of 1/2, so that both reactions differ only by the difference in the quantum Bose and Fermi distributions.

Integrals in Eqs. (33) and (34) can be evaluated in spherical coordinates. We define

$$q = p_1+p_2; \qquad p = \tfrac{1}{2}(p_1-p_2); \qquad q' = p_3+p_4; \qquad p' = \tfrac{1}{2}(p_3-p_4); \tag{38}$$

the z axis is chosen in the direction of $\vec{q} = \vec{p}_1 + \vec{p}_2$:

$$q_\mu = (q_0, 0, 0, 0), \qquad p_\mu = (p_0, p\sin\theta, 0, p\cos\theta),$$
$$p'_\mu = (p'_0, p'\sin\phi\sin\chi, p'\sin\phi\cos\chi, p'\cos\phi).$$

Now we obtain [10]:

$$R_{\substack{e\bar{e}\\ \gamma\gamma}\leftrightarrow\mu\bar{\mu}} = \frac{1}{1+I}\frac{(4\pi)(2\pi)}{(2\pi)^4 16}\int_{2m_\mu}^\infty dq_0\int_0^{s-q_0^2}dq\int_{-(q/2)}^{q/2}dp_0\int_{-(q^*/2)}^{q^*/2}dp'_0\int_0^\infty dp\int_0^\infty dp'\int_{-1}^1 d(\cos\theta)\int_{-1}^1 d(\cos\phi)$$
$$\times\int_0^{2\pi}d\chi\,\delta\left(p-\left(p_0^2+\frac{s}{4}\right)^{1/2}\right)\delta\left(p'-\left(p_0'^2-m_\mu^2+\frac{s}{4}\right)^{1/2}\right)\delta\left(\cos\theta-\frac{q_0p_0}{qp}\right)\delta\left(\cos\phi-\frac{q_0p'_0}{qp}\right)$$
$$\times\sum|M_{\substack{e\bar{e}\\ \gamma\gamma}\leftrightarrow\mu\bar{\mu}}|^2\Upsilon_\mu^{-2}f_\mu\left(\frac{q_0}{2}+p_0\right)f_\mu\left(\frac{q_0}{2}-p_0\right)\Upsilon_{\substack{e\\ \gamma}}^{-2}f_{\substack{e\\ \gamma}}\left(\frac{q_0}{2}+p'_0\right)f_{\substack{e\\ \gamma}}\left(\frac{q_0}{2}-p'_0\right)\exp(q_0/T), \tag{39}$$

where $q^* = q\sqrt{1-\frac{4m_\mu^2}{s}}$. The integration over p, p', $\cos\theta$, $\cos\phi$ can be done analytically considering the delta-functions. The other integrals can be evaluated numerically. For the case of indistinguishable colliding particles (two photons) there is an additional factor of 1/2 implemented by the value $I = 1$, while for distinguishable colliding particles (here electron and positron) $I = 0$.

C. $\pi^\pm$ production

$\pi^\pm$ can be produced in $\pi^0\pi^0$ charge exchange scattering,

$$\pi^0+\pi^0 \to \pi^+ + \pi^-, \tag{40}$$

as well as in two photon, and in electron-positron fusion processes

$$\gamma+\gamma \to \pi^+ + \pi^-, \tag{41}$$

$$e^+ + e^- \to \pi^+ + \pi^-. \tag{42}$$

We find that for π^0 density near to the chemical equilibrium, the last two $\pi^\pm$ production processes are much slower compared to the first process considered. Similarly, the two photon fusion to two π^0,

$$\gamma+\gamma \to \pi^0+\pi^0, \tag{43}$$

turns out, as expected, to be much smaller than one π^0 production. It is a reaction of higher order in α, and the energy is shared between two final particles.

The time evolution equations for the number of $\pi^\pm$ are similar to Eq. (29):

$$\frac{1}{V}\frac{dN_{\pi^\pm}}{dt} = (\Upsilon^2_{\pi^0} - \Upsilon^2_{\pi^\pm})R_{\pi^0\pi^0\leftrightarrow\pi^+\pi^-} + (\Upsilon^2_{\gamma} - \Upsilon^2_{\pi^\pm})R_{\gamma\gamma\leftrightarrow\pi^+\pi^-} + (\Upsilon^2_{e} - \Upsilon^2_{\pi^\pm})R_{e^+e^-\leftrightarrow\pi^+\pi^-}. \quad (44)$$

In order to evaluate the pion production rates in two body processes we use a reaction cross section, and the relation [14]

$$R_{12\leftrightarrow\pi^+\pi^-} = \frac{g_1 g_2}{32\pi^4}\frac{T}{1+I}\int_{s_{\rm th}}^{\infty} ds\sigma(s)\frac{\lambda_2(s)}{\sqrt{s}}K_1(\sqrt{s}/T) \quad (45)$$

[compared to Ref. [14] our definition is changed to $R_{12\to34} \to R_{12\to34}/(\Upsilon_1\Upsilon_2)$], where

$$\lambda_2(s) = (s-(m_1+m_2)^2)(s-(m_1-m_2)^2), \quad (46)$$

m_1 and m_2, g_1 and g_2, Υ_1 and Υ_2 are masses, degeneracy, and fugacities of initial interacting particles.

For the three cross sections we consider, we use, respectively (results valid in the common range $s \le 1$ GeV^2):

(i) The cross section for charge exchange π^0 scattering reaction Eq. (40) has been considered in depth recently [15]:

$$\sigma = \frac{16\pi}{9}\sqrt{\frac{s-4M^2_{\pi^\pm}}{s-4M^2_{\pi^0}}}(a_0^{(0)} - a_0^{(2)})^2, \quad (47)$$

where $a_0^{(0)} - a_0^{(2)} = 0.27/M_{\pi^\pm}$. This is the dominant process for charge pion production, subject to presence of π^0.

(ii) For process Eq. (41), the cross section of $\pi^\pm$ production in photon fusion, we use [16]

$$\sigma_{\gamma\gamma\to\pi^+\pi^-} = \frac{2\pi\alpha^2}{s}\left(1-\frac{4m_\pi^2}{s}\right)^{1/2} \times\left(\frac{m_V^4}{(1/2s+m_V^2)(1/4s+m_V^2)}\right), \quad (48)$$

where $m_V = 1400.0$ MeV. As we will see from numerical calculations given for the cross sections for $\gamma\gamma \to \pi^+\pi^-$, resulting production rates will be smaller than the charge exchange $\pi^0\pi^0 \to \pi^+\pi^-$ reaction.

(iii) For process Eq. (42), the cross section of $\pi^\pm$ production in electron-positron fusion, we use [17]

$$\sigma_{e^+e^-\to\pi^+\pi^-} = \frac{\pi\alpha^2}{3}\frac{(s-4m_\pi^2)^{3/2}}{s^{5/2}}|F(s)|^2. \quad (49)$$

The form factor $F(s)$ can be written in the form

$$F(s) = \frac{m_\rho^2 + m_\rho\Gamma_\rho d}{m_\rho^2 - s + \Gamma_\rho(m_\rho^2/k_\rho^3)[k^2(h(s)-h(m_\rho^2)) + k_\rho^2 h'(m_\rho^2)(m_\rho^2 - s)] - im_\rho(k/k_\rho)^3\Gamma_\rho(m_\rho/\sqrt{s})}, \quad (50)$$

where $h'(s) = dh/ds$ and

$$k = \left(\frac{1}{4}s - m_\pi^2\right)^{1/2}, \qquad k_\rho = \left(\frac{1}{4}m_\rho^2 - m_\pi^2\right)^{1/2},$$
$$h(s) = \frac{2}{\pi}\frac{k}{\sqrt{s}}\ln\left(\frac{\sqrt{s}+2k}{2m_\pi}\right),$$

$m_\rho = 775$ MeV, $\Gamma_\rho = 130$ MeV, $d = 0.48$. Given this cross section we also find that the rate of charged pion production is small when compared to π^0 charge exchange scattering.

(iv) For reaction (43) we have [18]

$$\sigma(\gamma\gamma\to\pi^0\pi^0) = \left(\frac{\alpha^2\sqrt{s-4m_\pi^2}}{8\pi^2\sqrt{s}}\right)\left[1+\frac{m_\pi^2}{s}f_s\right] \times\sigma(\pi^+\pi^-\to\pi^0\pi^0), \quad (51)$$

where

$$f_s = 2(\ln^2(z_+/z_-) - \pi^2) + \frac{m_\pi^2}{s}(\ln^2(z_+/z_-) + \pi^2)^2, \quad (52)$$

and $z_\pm = (1/2)(1 \pm \sqrt{s-4m_\pi^2})$.

The cross sections for $\pi^+\pi^-$ pair production, evaluated using Eqs. (47)–(49), are presented in Fig. 4 as functions of reaction energy $\sqrt{s}$. The top solid line (blue) is for charged pion production in π^0 scattering in Eq. (40), the magnitude of this cross section being so very large we reduce it in presentation by a factor of 1000; the dashed line is for $\pi^+\pi^-$ production in photon fusion in Eq. (41); the dash-dotted line is for electron-positron fusion in Eq. (42). The bottom solid line (green) is for photon fusion into two neutral pions, Eq. (51). The prediction for $\sigma_{\gamma\gamma\to\pi^+\pi^-}$ is about 480 nb (data 420 nb) at the peak near threshold [18], which is in agreement with calculations presented here. The reaction $\sigma_{\gamma\gamma\to\pi^0\pi^0}$[Eq. (43)] is much smaller than the others, and we do not consider this reaction further. We note that some of these results are currently under intense theoretical discussion as they relate to chiral symmetry. For

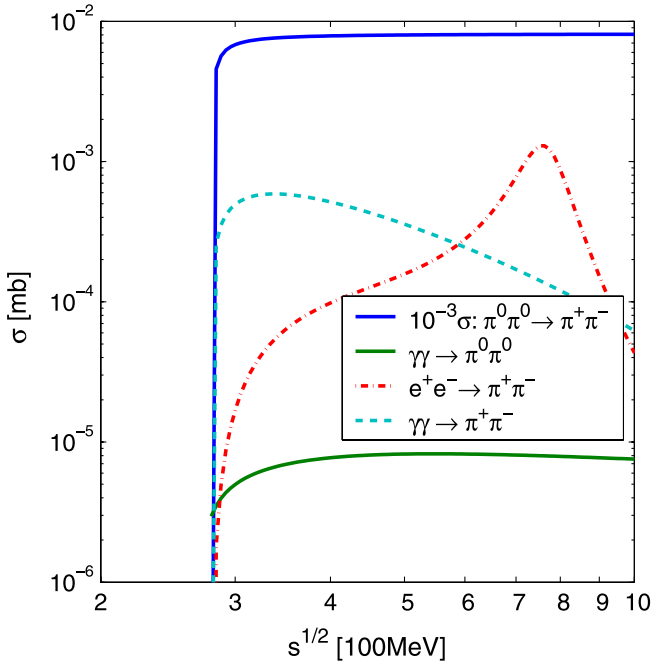

FIG. 4 (color online). The cross section σ for pion pair production, and pion charge exchange (solid top line), as functions of $\sqrt{s} \leq 1$ GeV^2.

our purposes the level of precision of here presented reaction cross sections is quite adequate.

III. NUMERICAL RESULTS

A. Particle production relaxation times

In Fig. 5 we show the relaxation time τ for the different processes considered as functions of temperature $T \in [3, 50]$ MeV. Because of the large difference in production rates which can be compensated by different densities of particles present (magnitudes of fugacities), we introduce the partial relaxation time for each of the three reactions $\pi^0\pi^0 \to \pi^+\pi^-$, $\gamma\gamma \to \pi^+\pi^-$, and $e^+e^- \to \pi^+\pi^-$:

$$\tau_{\pi^0\pi^0\leftrightarrow\pi^+\pi^-} = \frac{1}{2}\frac{dn_{\pi^\pm}/d\Upsilon_{\pi^\pm}}{R_{\pi^0\pi^0\leftrightarrow\pi^+\pi^-}};$$
$$\tau_{\gamma\gamma\leftrightarrow\pi^+\pi^-} = \frac{1}{2}\frac{dn_{\pi^\pm}/d\Upsilon_{\pi^\pm}}{R_{\gamma\gamma\leftrightarrow\pi^+\pi^-}}; \qquad (53)$$
$$\tau_{e^+e^-\leftrightarrow\pi^+\pi^-} = \frac{1}{2}\frac{dn_{\pi^\pm}/d\Upsilon_{\pi^\pm}}{R_{e^+e^-\leftrightarrow\pi^+\pi^-}}.$$

When $T \ll m$, we can use the Boltzmann approximation to the particle distribution functions. Since in this limit the density is proportional to Υ, the relaxation times do not depend on Υ. Moreover, even for $T \to 50$ MeV, we have for muons $e^{-m/T} \simeq 1/3$; thus quantum correlations in phase space remain small, and the Boltzmann limit can be employed. To account for a small quantum deviation

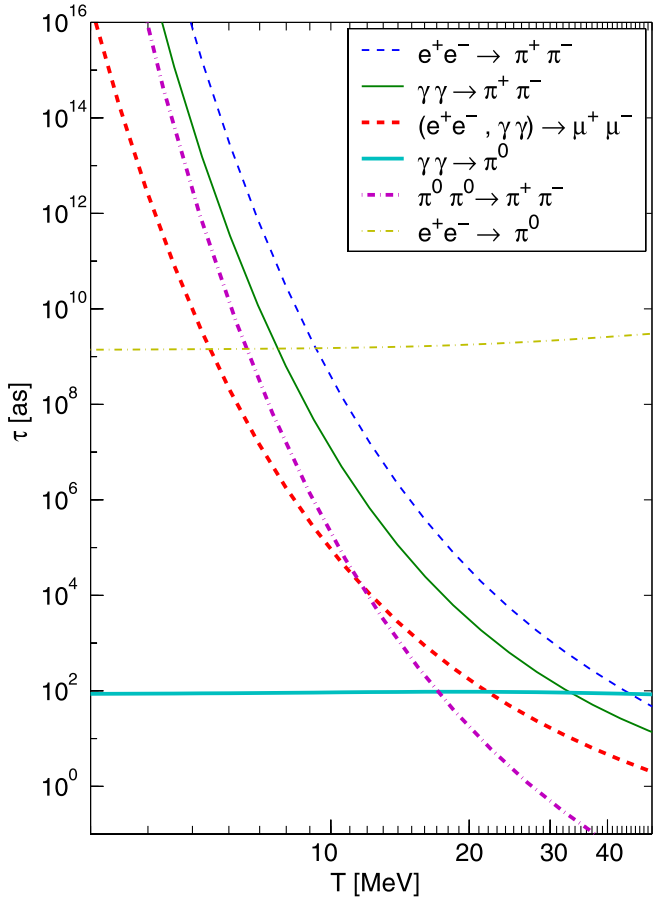

FIG. 5 (color online). The relaxation time τ for the different channels of pion and muon production (see box), as functions of plasma temperature T.

from the Boltzmann value arising especially at the upper limit $T \simeq 50$ MeV we consider, we evaluated τ using exact quantum statistics with $\Upsilon_i = 1$, this value corresponding to the maximum buildup of particle density at a given temperature, for which the quantum effect is largest. In addition to these three cases in Eq. (53) we show in Fig. 5 the muon production relaxation time of Eq. (30), the two photon fusion into π^0 relaxation time of Eq. (19), and a nearly horizontal line (bottom, turquoise), which is slightly greater than the free space π^0 decay rate. Finally, the thin dash-dotted line at about 10^8 times greater value of time is the electron-positron fusion into π^0, Eq. (12).

B. Rates of pion and muon formation

In Fig. 6 we show on the left as a solid (blue) line as a function of fireball temperature the rate per unit volume and time for the process $\gamma + \gamma \to \pi^0$, the dominant mechanism of pion production. The other solid line with dots corresponds to the $e^+ + e^- \to \pi^0$ reaction which in essence remains, in comparison, insignificant. Its importance follows from the fact that it provides the second-most-dominant path to π^0 formation at the lowest tem-

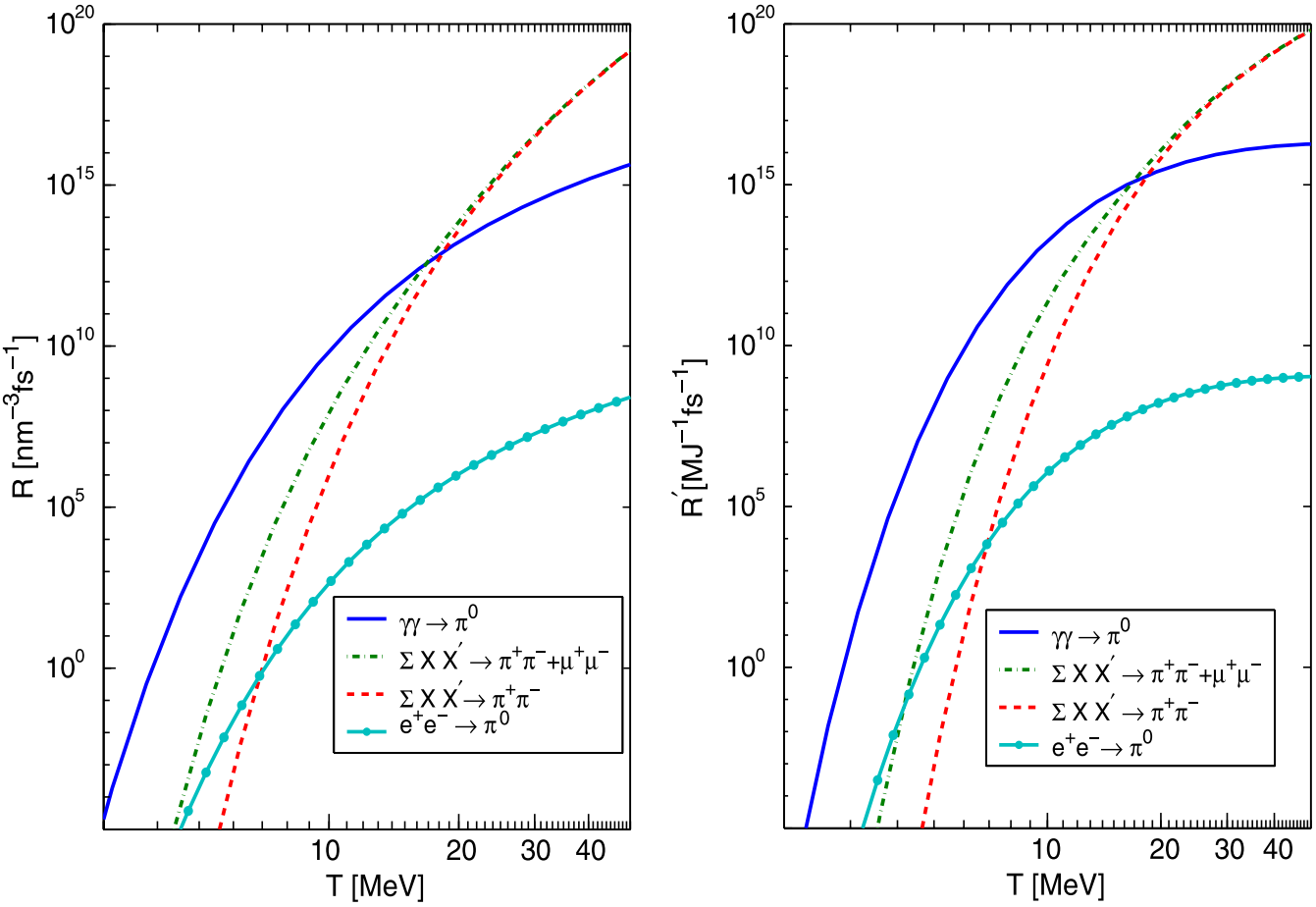

FIG. 6 (color online). On the left, the invariant pion production rates in units of $\mathrm{nm}^{-3}\,\mathrm{fs}^{-1}$, as a function of temperature T. On the right, the production rate R' per joule energy content in the fireball, in units of $\mathrm{MJ}^{-1}\,\mathrm{fs}^{-1}$. (In both cases for reactions shown in the box.)

peratures considered, and it operates even if and when photons are not confined to remain in the plasma drop.

We improve the rate presentation on the right-hand side in Fig. 6: considering that the formation of a plasma state involves an experimentally given fireball energy content $\mathcal{E}$ in joules, we use Eq. (6) to eliminate the volume V at each temperature T:

$$R'_{\pi^0} \equiv \frac{d^2W'_{\gamma\gamma\to\pi^0}}{dtd\mathcal{E}} = \frac{1}{g\sigma T^4}\frac{d^4W_{\gamma\gamma\to\pi^0}}{dVdt} = \frac{1}{g\sigma T^4}R_{\pi^0}. \tag{54}$$

For chemical nonequilibrium, replace $g \to \Upsilon_\gamma^2 g(\Upsilon)$. Considering the (good) approximate Eq. (21) we obtain

$$R'_{\pi^0} \simeq \left(\frac{m_\pi}{2\pi T}\right)^{3/2}\frac{e^{-m_\pi/T}}{g\sigma T\tau^0_{\pi^0}}. \tag{55}$$

We use units such that $\hbar = 1$, $c = 1$, $k = 1$, and thus R' is a dimensionless expression. Recalling the value of these constants, the units we used for R' derive from $\mathrm{MeV\,s} = 1.603\,10^{-4}$ MJ fs.

The other lines in Fig. 6 address the sum of formation rates of charged pion pairs (dashed, red) by all reactions considered in this work, $\pi^0 + \pi^0 \to \pi^+ + \pi^-$, $\gamma + \gamma \to \pi^+ + \pi^-$, $e^+ + e^- \to \pi^+ + \pi^-$. We also present the sum of all reactions leading to either a charged pion pair or a muon pair (dash-dotted line, green), that is, the sum of $\gamma + \gamma \to \mu^+ + \mu^-$, $e^+ + e^- \to \mu^+ + \mu^-$. The rationale for this presentation is that we do not care how a heavy particle is produced, as long as it can be observed. The dashed (red) line assumes that we specifically look for charged pions, and the dash-dotted (green) line that we wait till charged pions decays, being interested in the total final muon yield. The π^0 production rate (solid line, blue) is calculated using Eq. (16) and yields on the logarithmic scale a nearly indistinguishable result from the approximation of Eq. (21). For $\pi^\pm$ production we refer to Sec. II C and for $\mu^\pm$ production we refer to Sec. II B.

In Table I we show the values of key reaction rates R and relaxation times τ at $T = 5$ and 15 MeV. We note the

TABLE I. Values of rates, relaxation times for all reactions at $T = 5$ MeV and $T = 15$ MeV.

Reaction	$T = 5$ MeV τ [as]	$T = 5$ MeV R [nm^{-3} fs^{-1}]	$T = 15$ MeV τ [as]	$T = 15$ MeV R [nm^{-3} fs^{-1}]
$\gamma\gamma \leftrightarrow \pi^0$	88	$3.3\,10^{3}$	95	$1.2\,10^{12}$
$e^+e^- \leftrightarrow \mu^+\mu^-$	$1.2\,10^{10}$	$3.2\,10^{-3}$	$1.9\,10^{3}$	$1.5\,10^{11}$
$\gamma\gamma \leftrightarrow \mu^+\mu^-$	$1.0\,10^{10}$	$3.7\,10^{-3}$	$1.3\,10^{3}$	$2.1\,10^{11}$
$\pi^0\pi^0 \leftrightarrow \pi^+\pi^-$	$2.9\,10^{12}$	$2.1\,10^{-8}$	$4.6\,10^{2}$	$9.5\,10^{10}$
$\gamma\gamma \leftrightarrow \pi^+\pi^-$	$6.4\,10^{13}$	$9.7\,10^{-10}$	$5.1\,10^{4}$	$8.7\,10^{8}$
$e^+e^- \leftrightarrow \pi^+\pi^-$	$7.8\,10^{15}$	$7.9\,10^{-12}$	$9.5\,10^{5}$	$4.6\,10^{7}$

extraordinarily fast rise of the rates with temperature, in some instances bridging 15–20 orders in magnitude when results for $T = 5$ and 15 MeV are compared.

In order to understand the individual contributions to the different reactions entering the sum of rates presented above, we show as a function of temperature in Fig. 7 the relative strength of the muon pair (left) and charge pion (right) electromagnetic ($\gamma + \gamma, e^+ + e^-$) production, using as the reference the $\gamma + \gamma \rightarrow \pi^0$ reaction. The $\mu^{\pm}$ production rates are calculated using Eq. (39) with $|M|^2$ from Eqs. (35) and (36), respectively. This ratio is smaller than unity for $T \lesssim 20$ MeV. For larger T, the muon direct production rate becomes larger than the π^0 production rate. Charged pions (on right in Fig. 7) can be produced in direct reaction at a rate larger than neutral pions only for $T >$ 35 MeV. The photon channel dominates.

IV. DISCUSSION AND CONCLUSIONS

We found that the production of π^0 is the dominant coupling of electromagnetic radiation to heavy (hadronic) particles with $m \gg T$ and, as we have here demonstrated, that noticeable particle yields can be expected already at modest temperatures $T \in [3, 10]$ MeV. In the present-day environment of 0.1 and up to one kJ plasma lasting a few fs, our results suggest that we can expect integrated over space-time evolution of the EP^3 fireball a π^0 yield at the limit of detectability. For $T \rightarrow 15$ MeV the π^0 production rate remains dominant and indeed very large, reaching the

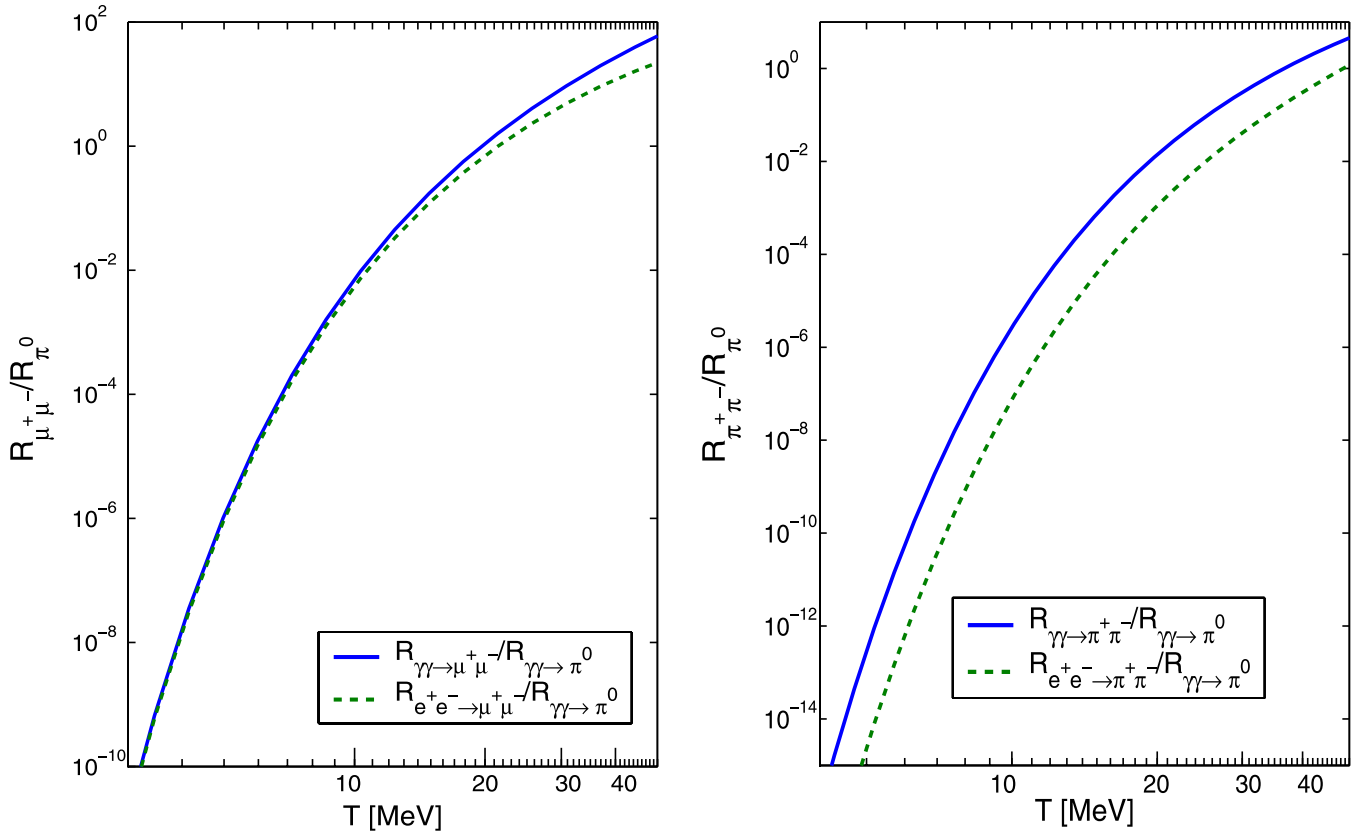

FIG. 7 (color online). On left, muon and, on right, charged pion production rates in electromagnetic processes normalized by the π^0 production rate. The solid line (blue) is for the $\gamma\gamma$ and the dashed line (green) for the e^+e^- induced process.

production rate $R' \simeq 10^{15}$ [MJ^{-1} fs^{-1}]. Charge exchange reactions convert some of the neutral pions into charged pions which are more easy to detect.

In this situation it is realistic to consider the possibility of forming a chemically equilibrated fireball with π^0, $\pi^\pm$, $\mu^\pm$ in chemical abundance equilibrium. The heavy particles are produced in early stages when temperature reached is highest. Their abundance in the fireball follows the fireball expansion and cooling till their freeze-out, that is, decoupling of population equation production rates. The particle yields are then given by the freeze-out conditions, specifically the chemical freeze-out temperature T_f and volume V_f, rather than the integral over the rate of production. In this situation the heavy particle yields become diagnostic tools of the freeze-out conditions, with the mechanisms of their formation being less accessible. However, one can avoid this condition by appropriate staging of fireball properties.

The present study has not covered, especially for the low temperature range all the possible mechanisms, and we addressed some of these issues in the introduction. Here we note further that the production of heavy particles requires energies of the magnitude $m/2$ and thus is due to collisions involving the (relatively speaking) far tails of a thermal particle distribution. If these tails fall off as a power law, instead of the Boltzmann exponential decay [19], a much greater yield of heavy particles could ensue. There could further be present a collective amplification to the production process, e.g., by residual matter flows, capable of enhancing the low temperature yields, or by collective plasma oscillations and inhomogeneities.

These are just some examples of many reasons to hope for and expect a greater particle yield than we computed here in a microscopic and controllable two particle reaction approach. This consideration, and our encouraging ''conventional'' results, suggest that the study of π^0 formation in QED plasma is of considerable intrinsic interest. Our results provide a lower limit for the rate of particle production and, when folded with models of EP^3 fireball formation and evolution, final yield.

It is of some interest to note that the study of pions in QED plasma allows exploration of pion properties in electromagnetic medium. Specifically, recall that 1.2% fraction of $\pi^0 \to e^+e^-\gamma$ decays, which implies that the associated processes such as $e^+ + e^- \to \gamma + \pi_0$ are important. We cannot evaluate this process at present as it involves significant challenges in understanding of π^0 off-mass shell ''anomalous'' coupling to two photons.

The experimental environment we considered here should allow a detailed study of the properties of pions (and also muons) in a thermal background. There is considerable fundamental interest in the study of pion properties and specifically pion mass splitting in QED plasma at temperature $T \gtrsim \Delta m$ and in the presence of electromagnetic fields. We already have shown that due to quantum statistics effects, the effective in-medium decay width of π^0 differs from the free space value (see Fig. 2). In addition, modification of mass and decay width due to ambient medium influence on the pion internal structure is to be expected. Further we hope that the study of pions in the EP^3 fireball will contribute to the better understanding of the relatively large difference in mass between π^0 and $\pi^\pm$. The relatively large size of the PE^3 environment should make such changes, albeit small, measurable.

The experimental study of π^0 in the QED plasma environment is not an easy task. Normally, one would think that the study of the π^0 decay into two 67.5 MeV γ (+ thermal Doppler shift motion) produces a characteristic signature. However, the π^0 decay is in time and also in location overlapping with the plasma formation and disintegration. The debris of the plasma reaches any detection system at practically the same time instance as does the 67.5 MeV γ. The large amount of available radiation will disable the detectors. On the other hand we realize that the hard thermal component of the plasma, which leads to the production of π^0 in the early fireball stage, is most attenuated by plasma dynamical expansion. Thus it seems possible to plan for the detection of π^0, e.g., in a heavily shielded detection system.

The decay time of charged pions being 26 ns, and that of charged muons being 2.2 μs, it is possible to separate in time the plasma debris from the decay signal of these particles. Clearly, these heavy charged particles can be detected with much greater ease, also considering that the decay product of interest is charged. For this reason, we also have in depth considered all channels of production of charged pions and muons. Noting that practically all charged pions turn into muons, we have also compared the production rates of π^0 with all heavy particles [see dashed (green) line in Fig. 7]. This comparison suggests that for plasmas at a temperature reaching $T > 10$ MeV the production of final state muons will most probably be easier by far to detect. On the other hand for $T < 5$ MeV it would seem that the yield difference in favor of π^0 outweighs the detection system/efficiency loss considerations. Future work addressing nonconventional processes will show at how low a T we can still expect observable heavy particle yields.

An effort to detect π^0 directly is justified since we can learn about the properties of the plasma (lifespan, volume, and temperature in early stages), e.g., from a comparative study of the π^0 and $\pi^\pm$ production. We have found that at about $T > 16$ MeV, the pion charge exchange $\pi^0\pi^0 \to \pi^+\pi^-$ reaction for chemically equilibrated π^0 yield is faster than the natural π^0 decay and the chemical equilibration time constant (see the steeply descending dash-dotted line in Fig. 5). Thus beyond this temperature the yield of charged pions can be expected to be in/near chemical equilibrium for a plasma which lives at or above this temperature for longer than 100 as.

In such an environment the yield of π^0 is expected to be near chemical equilibrium, since the decay rate is compensated by the production rate, and within 100 as, the chemical equilibrium yield is attained. Moreover, the thermal speed of produced π can be obtained from the nonrelativistic relation $\frac{1}{2}m\langle v^2\rangle = \frac{3}{2}T$; thus $\bar{v} \propto \sqrt{T}$ and, for $T = 10$ MeV, $\overline{v} \simeq 0.5c$. This is nearly equal to the sound velocity of EP^3, $v_s \simeq c/\sqrt{3} = 0.58c$. Thus the heavy π^0 particles can be seen as comoving with the expanding/exploding EP^3, which completes the argument to justify their transient chemical equilibrium yield in this condition.

The global production yield of neutral and charged pions should thus allow the study of volume and temperature history of the QED plasma. More specifically, since with decreasing temperature, for $T < 16$ MeV, there is a rapid increase of the relaxation time for the charge exchange process, there is a rather rapid drop of the charged pion yield below chemical equilibrium—we note that charge exchange equilibration time at $T = 10$ MeV is a factor of 10^5 longer. We note that the study of two pion correlations provides an independent measure of the source properties (Hanbury-Brown, Twiss measurement).

The relaxation time of the electromagnetic production of muon pairs wins over the π^0 relaxation time for $T > 22$ MeV (see lower dashed line, red, in Fig. 5); the direct electromagnetic processes of charged pion production (thin solid line, green, for $\gamma\gamma \rightarrow \pi^+\pi^-$ and dashed line, blue, for $e^+e^- \rightarrow \pi^+\pi^-$) remain subdominant. Thus for $T > 22$ MeV we expect, following the same chain of arguments for muons as above for charged pions, a near chemical equilibrium yield. If the study of all these π^0, $\pi^\pm$, $\mu^\pm$ yields and their spectra, and even pion correlations were possible, considerable insight into e^-, e^+, γ plasma (EP^3) plasma formation and dynamics at $T < 25$ MeV can be achieved.

ACKNOWLEDGMENTS

This research was supported by the DFG Cluster of Excellence: Munich Center for Advanced Photonics and by U.S. Department of Energy Grant No.DE-FG02-04ER4131.

Note added in proof.—After completion of this work we learned about a study of chemical equilibration of $e, \bar{e}, \gamma$ components in EP^3 in temperature domain $0.1 \leq T \leq 10$ MeV [20]. Its qualitative results are consistent with our use of chemically equilibrated $e, \bar{e}, \gamma$ in the study of pion and muon production.

[1] T. Tajima and G. Mourou, Phys. Rev. ST Accel. Beams **5**, 031301 (2002).
[2] T. Tajima, G. Mourou, and S. V. Bulanov, Rev. Mod. Phys. **78**, 309 (2006).
[3] M. H. Thoma, arXiv:0801.0956.
[4] See, for example, the introduction in E. M. Lifshitz and L. D. Landau, *Statistical Physics*, Course of Theoretical Physics Vol. 5 (Butterworth-Heinemann, Oxford, UK, 1984).
[5] Baifei Shen and J. Meyer-ter-Vehn, Phys. Rev. E **65**, 016405 (2001).
[6] M. H. Thoma (private communication).
[7] I. Kuznetsova, T. Kodama, and J. Rafelski, "Chemical Equilibration Involving Decaying Particles at Finite Temperature" (unpublished).
[8] T. Biro and J. Zimanyi, Phys. Lett. B **113**, 6 (1982).
[9] J. Rafelski and B. Muller, Phys. Rev. Lett. **48**, 1066 (1982); **56**, 2334(E) (1986).
[10] T. Matsui, B. Svetitsky, and L. D. McLerran, Phys. Rev. D **34**, 783 (1986); **37**, 844(E) (1988).
[11] P. Koch, B. Muller, and J. Rafelski, Phys. Rep. **142**, 167 (1986).
[12] B. L. Combridge, Nucl. Phys. **B151**, 429 (1979).
[13] M. Gluck, J. F. Owens, and E. Reya, Phys. Rev. D **17**, 2324 (1978).
[14] J. Letessier and J. Rafelski, *Hadrons and Quark-Gluon Plasma*, Cambridge Monogr. Part. Phys., Nucl. Phys., Cosmol. Vol. 18 (Cambridge University Press, Cambridge, UK, 2002), p. 1.
[15] R. Kaminski, J. R. Pelaez, and F. J. Yndurain, Phys. Rev. D **77**, 054015 (2008).
[16] H. Terazawa, Phys. Rev. D **51**, R954 (1995).
[17] G. J. Gounaris and J. J. Sakurai, Phys. Rev. Lett. **21**, 244 (1968).
[18] G. Mennessier, P. Minkowski, S. Narison, and W. Ochs, arXiv:0707.4511, in *Proceedings of the Third High-Energy Physics International Conference (HEPMAD07) Antananarivo, Madagascar; September 10–15, 2007*, http://www.slac.stanford.edu/econf/C0709107.
[19] T. S. Biro and A. Jakovac, Phys. Rev. Lett. **94**, 132302 (2005).
[20] A. G. Aksenov, R. Ruffini, and G. V. Vereshchagin, Phys. Rev. Lett. **99**, 125003 (2007).